

Journal Pre-proof

Radiological emergency dosimetry – The use of luminescent mineral fillers in polymer-based fabrics

Lily Bossin, Ian Bailiff, Ian Terry

PII: S1350-4487(20)30082-2

DOI: <https://doi.org/10.1016/j.radmeas.2020.106318>

Reference: RM 106318

To appear in: *Radiation Measurements*

Received Date: 16 December 2019

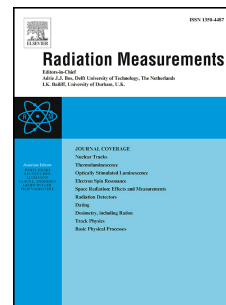
Revised Date: 16 March 2020

Accepted Date: 19 March 2020

Please cite this article as: Bossin, L., Bailiff, I., Terry, I., Radiological emergency dosimetry – The use of luminescent mineral fillers in polymer-based fabrics, *Radiation Measurements* (2020), doi: <https://doi.org/10.1016/j.radmeas.2020.106318>.

This is a PDF file of an article that has undergone enhancements after acceptance, such as the addition of a cover page and metadata, and formatting for readability, but it is not yet the definitive version of record. This version will undergo additional copyediting, typesetting and review before it is published in its final form, but we are providing this version to give early visibility of the article. Please note that, during the production process, errors may be discovered which could affect the content, and all legal disclaimers that apply to the journal pertain.

© 2020 Published by Elsevier Ltd.



1 Radiological emergency dosimetry – the use of luminescent mineral fillers in
2 polymer-based fabrics

3 Lily Bossin^{*1,2,3}, Ian Bailiff¹ and Ian Terry²

4 * Current address: Institute of Earth Surface Dynamics, University of Lausanne, Lausanne,
5 Switzerland

6 ¹ Department of Archaeology, Durham University, Durham, UK

7 ² Department of Physics, Durham University, Durham, UK

8 ³ Public Health England, Radiation Metrology group, Didcot, UK

9
10 **Abstract**

11 Mineral fillers are widely used in the manufacture of thermoplastics and they are commonly found
12 in the fabrics used to form bags. We show that carbonate mineral filler grains incorporated within
13 faux leather fabrics and the coatings applied to woven nylon fibre fabrics exhibit a bright
14 thermoluminescence TL response to ionising radiation dose, similar to that of calcite, with a broad
15 thermoluminescence (TL) peak at 100 °C. The fabrics tested are shown to be potentially suitable as a
16 surrogate material for emergency dosimetry, exhibiting a linear TL response to dose between 0.1
17 and 10 Gy, and with a detection limit varying with fabric type from 4 to 400 mGy. The region of the
18 TL glow curve selected for dose evaluation was between ca 100 to 200 °C, and this is restricted by
19 the presence of a native signal associated with the 250 °C TL peak. The rate of fading observed
20 varied with glow curve temperature, attributed to the presence of a distribution of trapping levels;
21 following 24 h storage at room temperature the loss recorded for the optimal glow curve
22 temperature region selected (160-162 °C) ranged from 30 to 80%, according to fabric and filler type.
23 However, the fading mechanism is predominantly thermal and its rate can be substantially reduced
24 by storing irradiated materials below room temperature. The use of filler minerals incorporated in
25 the manufacture of plastics provides the scope to exploit a much wider range of materials for
26 application to emergency dosimetry.

27 **1. Introduction**

28 Following a radiological emergency affecting members of the public, prompt dose assessment is
29 needed to support the medical triage of individuals (Coleman et al., 2011; Ainsbury et al., 2010;
30 Bailiff et al., 2016). Luminescence techniques developed to respond to this need can be applied to
31 measure the absorbed dose resulting from exposure to gamma radiation using surface mount
32 components and screen glass in mobile communication devices (Inrig et al., 2008; Bassinet et al.,
33 2014). In particular, alumina substrates of resistors have been shown to have suitable
34 characteristics as dosimeters (low detection limit, linearity of the dose response; Ekendhal and
35 Judas, 2011; Kouroukla, 2015). However, their practical use in an emergency may be limited by the
36 reluctance of owners to surrender mobile phones for destructive testing, and also by the progressive
37 diminution in the number and size of surface mount components found in modern mobile phones.
38 Hence, the search continues for alternative materials that can be used as dosimeters in a radiological
39 emergency. Amongst a range of potentially suitable alternative materials, synthetic polymer-based
40 fabrics have the advantage of being available at various locations covering the body rather than at a
41 singular location, as is the case with a smart phone. In previous work Bossin et al. (2017) found that
42 certain types of polymer fibres have luminescent characteristics that are potentially suitable for
43 dosimetry measurements, although the mean lifetime of trapped charge within the polymer
44 structure was found to be too short for reliable determinations over a period of at least several days.
45 However, the fabrication process of many polymer-based materials (Wypych, 2016), in particular
46 fabrics, frequently includes the incorporation of mineral fillers, which typically comprise crushed
47 carbonate rock. Although the use of a silica filler in the epoxy encapsulation of chips in bank and ID
48 cards was demonstrated to be suitable for dosimetry in earlier work (Woda et al, 2012), mineral
49 fillers incorporated in the manufacture of polymer-based materials do not appear to have been
50 investigated as luminescent dosimeters. In this paper we examine the luminescent properties of
51 calcium carbonate fillers and assess whether fabrics containing them are potentially suitable for
52 deployment as a dosimeter in a radiological emergency.

53

54 *Carbonate fillers in polymer-based materials*

55 Mineral fillers are commonly incorporated in polymer-based materials to reduce the costs of
56 manufacture and to improve their physical characteristics to suit their particular function, such as
57 heat resistance, stiffness, abrasion resistance and biodegradability (Katz and Mileski, 1987; Wypych,
58 2016). The most widely used mineral is ground limestone, whose crystalline form, calcite, is a well-
59 studied luminescent material, emitting bright thermoluminescence (TL) attributed to the presence of
60 Mn (Medlin, 1959; Sunta, 1984; Kirsh et al., 1987) that appears to be ubiquitous amongst
61 sedimentary rocks (Medlin, 1968). The TL glow curve of calcite contains dominant peaks at ca 90 °C
62 and 235 °C ($0.5\text{ °C}\cdot\text{s}^{-1}$); in earlier work the former was reported to be associated with a continuum or
63 distribution of trapping levels (Medlin, 1959; Kirsh, 1987; Pagonis et al., 1996), although a simpler
64 model involving discrete traps has been adopted in more recent work (Kalita and Wary, 2014). The
65 TL emission spectrum is attributed primarily to recombination at Mn-defect complexes and contains
66 a dominant band located within the range ca 550- 650 nm, but may also contain emission bands at
67 shorter wavelengths (e.g., 460 nm) arising from other permitted transitions from the excited states
68 of Mn^{2+} (Down et al., 1985; Townsend et al., 1994). Although OSL has not been observed with calcite
69 (Galloway, 2002), possibly due to the low optical cross sections of the electron traps (Schulman et
70 al., 1947), studies of the optical bleaching behaviour of the higher temperature TL peaks (280 and
71 350 °C, $4\text{ °C}\cdot\text{s}^{-1}$) have found that charge in traps associated with these peaks can be optically
72 evicted by exposure of natural calcites to daylight (Kim and Hong, 2014; Liritzis et al, 1996). As these
73 studies focused on potential application to archaeological dating, the optical bleaching behaviour of
74 peaks present in the TL glow curve associated with thermally unstable traps has received less
75 attention. However, in the earlier work by Liritzis et al. (1996), the 130 °C TL peak ($4\text{ °C}\cdot\text{s}^{-1}$) present in
76 their glow curve exhibited markedly different bleaching characteristics, requiring short UV radiation
77 to obtain a significant reduction in the TL signal.

78

79 **2. Experimental**80 *Samples*

81 The samples examined comprised a set of 16 polyurethane-coated woven nylon-fibre swatches of
82 differing colours from the same manufacturer and a total of 21 used faux leather handbags, nylon
83 fabric backpacks and conference bags (Table S1, Supplementary Material) produced by different
84 manufacturers. In the case of backpacks and conference bags, a polyurethane thermoplastic layer
85 coating, commonly bonded to the inner surfaces of woven nylon fabric, contained the filler grains.
86 The faux-leather handbags tested were constructed with a thermoplastic polyurethane sheet fabric
87 containing the filler. Samples for measurements were cut as squares to fit into ca 10 mm diameter
88 stainless steel measurement cups designed for use in the luminescence reader; unless indicated
89 otherwise, the fabric surface was wiped to remove dust, but not altered by abrasion, for example.

90

91 *Instrumentation*

92 Thermoluminescence (TL) measurements were performed using a Risø model 12 reader (DTU
93 Nutech, Denmark) that incorporated a $^{90}\text{Sr}/^{90}\text{Y}$ radiation source. The luminescence was detected
94 using either of two types of photomultiplier (PMT) operated in single photon counting mode, with
95 various optical filter combinations inserted into the detection system: a) an Electron Tubes 9235
96 UV/blue sensitive PMT in combination with a UV pass colour glass filter (U-340) or a fused silica
97 window, or b) a Hamamatsu R2949 red sensitive PMT, in combination with either a fused silica
98 window, or with a sharp cut-off colour glass filter (selected with various long-pass wavelengths, 175-
99 700 nm as indicated in Fig. S1, Supplementary Material). The TL glow curves were recorded to a
100 maximum temperature of 200 °C to avoid thermal decomposition of the polymer and the generation
101 and distribution of volatile products in the measurement chamber, and a heating rate of $0.5\text{ °C}\cdot\text{s}^{-1}$
102 was employed to reduce thermal lag effects caused by the thickness of the fabrics (300-1200 μm). All

103 TL measurements were repeated at least twice with samples from different parts of the examined
104 item (e.g., front, back, side, inside pockets in the case of a bag) to test for uniformity of response of
105 the fabric.

106 The dose rate delivered by the $^{90}\text{Sr}/^{90}\text{Y}$ β source to calcium carbonate filler grains in the surface of
107 the fabric was estimated to be $0.86 \pm 0.04 \text{ Gy} \cdot \text{min}^{-1}$. The latter was derived from the measured dose
108 rate to grains of quartz distributed on the upper surface of fabric samples of different thickness
109 placed in stainless steel cups, where the quartz had been irradiated with a known gamma dose.

110 Elemental, topographical and cathodoluminescence imaging analysis of samples was performed
111 using a Hitachi SU-70 scanning electron microscope (SEM), with additional facilities providing
112 cathodoluminescence spectroscopy (Gatan Mono-CL cathodoluminescence) and imaging (Pixis CCD
113 camera) and energy-dispersive X-ray (EDX) spectroscopy. X-ray diffraction (XRD) measurements were
114 performed using a Bruker AXS D8 Advance equipped with a Lynxeye Soller PSD detector (See also
115 Section 1, Supplementary Material).

116 **3. Material characterisation**

117 The presence of grains of the mineral filler was initially identified visually in the PU coating of the
118 nylon fabric of backpacks and conference bags (Fig. 1). Subsequent examination using a SEM (Fig. 2)
119 revealed that the grains were loosely bonded within the PU film and ranged in size from ca 10 to ca
120 $100 \mu\text{m}$; the presence of angular edges indicated freshly pulverised rock. The XRD patterns obtained
121 with samples of filler grains taken from the three types of bag identified them as a carbonate, the
122 components of the diffraction patterns matching well with a sourced mineral calcite (Fig. 3).
123 Additional energy dispersive XRF (EDX) measurements indicated the presence of magnesium
124 limestone (dolomite) and accessory minerals (e.g., sand or chert; Folk, 1962) in some samples (Fig.
125 3d). Measurements with samples taken from different locations of bags or fabric swatches
126 confirmed qualitatively a uniform distribution of fillers, although the proportion of filler in different
127 thermoplastics was observed to vary. Cathodoluminescence (CL) imaging (Fig. 4a) confirmed the

128 filler grains to be the dominant source of luminescence, and that the luminescence from the PU film
129 and polymer fibres was relatively much weaker. The CL emission spectrum (Fig. 4b) is both broad
130 and complex, containing, amongst several broad emission bands, a dominant peak at ~680 nm which
131 is similar to the characteristic orange-red emission of calcite (Down et al., 1985).

132 **4. Luminescence dose response**

133 As anticipated, none of the samples exhibited a measurable OSL response under blue (470 nm) or
134 infrared (850 nm) stimulation and consequently the TL emission was measured for all the samples
135 tested in this work. The TL glow curve measured with calcium carbonate filler grains (Fig. 5, curve c)
136 resembles that obtained with crushed limestone (Fig. 5, curve a), and this is consistent with the
137 compositional analysis discussed above. Measurement of the TL glow curve using different long pass
138 sharp-cut optical filters (Supplementary Material, Fig. S1) in the detection system confirmed the
139 presence of a dominant red band in the TL emission spectrum. The TL intensity was optimised (Fig.
140 6) by installing the red-sensitive PMT (Hamamatsu R2949) coupled with sharp cut filter OC12 (550
141 nm), which produced a TL signal that was ~50% stronger compared with that measured using the
142 blue sensitive PMT (EMI 9235) coupled with the same optical filter. The use of this detection
143 configuration also significantly attenuated a native TL signal that was observed in some unirradiated
144 samples (Fig. 7) where the detection window extended into the blue-green region of the spectrum
145 (Further details in Supplementary Material, Section 4).

146 The dose response of all except 3 of the 21 samples taken from the three types of bags and fabric
147 swatches tested exhibited a TL glow curve, measured to 200 °C, that was similar in shape, containing
148 two broad peaks centred at ca 25 and 100 °C ($0.5 \text{ }^\circ\text{C}\cdot\text{s}^{-1}$; Fig 5b). The TL glow curve measured with
149 filler grains extracted from the same fabric (Fig. 5b) indicates a stretching of the form of the glow
150 curve at higher temperatures arising from thermal lag. The position of the 100 °C TL peak was also
151 found to vary within ~15 °C between samples (Supplementary Material, Fig. S2), also attributed to
152 the presence of thermal lag, the extent of which is expected to be dependent on both the thickness

153 of fabric and the degree of contact with the underlying measurement pan. This interpretation is
154 supported qualitatively by the results of spatially-resolved TL measurements (Supplementary
155 Material, Fig. S3) with cut fabric samples, and also those by measurements with quartz grains placed
156 on the fabric surface as part of the β source calibration which indicated movement in the position of
157 the 110 °C TL peak of between 5 and 15 °C for different fabrics. Nonetheless, TL measurements with
158 samples cut from different parts of the fabric (e.g., front, back, side, inside pockets in the case of a
159 bag) indicated a general uniformity of TL response. Some dependency of TL sensitivity on fabric
160 colour was observed, with white and red coloured samples having the highest TL sensitivity to dose
161 (e.g., HB16PU, F179PUN, HB19PU). A separate investigation of the electron paramagnetic resonance
162 (EPR) spectra of two of the three samples mentioned above that did not produce a measurable TL
163 signal indicated negligible Mn^{2+} , in contrast to the other samples included in the study.

164
165 A linear TL dose response within the range of interest (0.1-10 Gy) was observed with bag and fabric
166 swatch samples, as shown in Fig. 8 for the TL glow curve integration ranges 105-135 °C, 140-160 °C
167 and 160-175 °C. The average value of the dose intercept was 20 ± 60 mGy (standard deviation from
168 12 samples; see also Supplementary Material Fig. S4). The detection limit, evaluated by calculating
169 the dose for which the signal was equal to the background plus three times the standard deviation of
170 the background, varied widely according to TL sensitivity. Amongst the brighter samples, the
171 detection limit for the 140-160 °C glow curve integral was a few mGy, whereas it approached 400
172 mGy for the least sensitive sample taken from a black faux leather handbag (HB10PUN).

173 **5. Fading**

174 Fading tests were performed by administering a 10 Gy β dose to samples, followed by storage at
175 ambient temperatures in dark conditions for periods ranging from 0.5 to 744 h. The TL glow curves
176 recorded following storage exhibited a progressive shift of the peak maximum to higher
177 temperatures with increasing storage time, as illustrated in Fig. 9 for the first 24 h of storage. The

178 consequent change in fading rate with glow curve temperature required the use of narrow
179 integration intervals (2 °C) in the analysis of the TL data. An example of fading behaviour at ambient
180 temperatures measured with a sample of PU coated woven nylon fabric (F179PUN) is shown in Fig.
181 10 for two glow curve intervals (140-142 °C and 158-160 °C). The form of reduction was fitted with a
182 stretched exponential function for all the samples tested; the rate of loss varied widely between
183 samples, as indicated in Fig. 11 where increasing dispersion in the proportions of remaining TL with
184 storage time is evident. To retain at least half the initial signal after storage at ambient temperatures
185 required the use of glow curve integration regions above 140 °C. Tests of optical fading under white
186 fluorescent lighting for periods up to 5 h indicated negligible depletion of the TL signal compared
187 with that obtained following storage under dark conditions. Fading tests were also performed with a
188 subset of samples at storage temperatures of -15 °C (7 samples) and at 35 °C (2 samples), an
189 example of which is shown in Fig 12 for a sample of PU coated nylon fabric (F179PUN) stored at -15
190 °C. The TL remaining (158-160 °C glow curve interval) after 183 days of storage was 60% of the initial
191 signal, whereas equivalent measurements with the same fabric performed at storage temperatures
192 of RT and 35 °C yielded values of 25% and 7% TL remaining, respectively, after 24 h of storage. The
193 extent of variation in fading rates between samples stored at these two temperatures was
194 comparable to that observed at ambient temperatures for longer storage periods (e.g. >10 days). On
195 the basis of the results of fading tests performed at different storage temperatures, the dominant
196 mechanism of charge loss for the samples tested was interpreted to be governed by a thermally
197 assisted escape of trapped charge. Using the results of the fading tests performed at the three
198 storage temperatures, values of activation energy and frequency factor were estimated by
199 constructing Arrhenius plots for the two TL glow curve intervals examined above, 140-142 °C and
200 158-160 °C (Table 1), yielding estimates of trap depth of 0.8 and 0.9 eV for these two temperature
201 intervals respectively.

202 6. Investigation of trap depth

203 The observation of a progressive increase in the temperature of the TL glow curve maximum with
204 storage time, together with the strong change in the rate of fading with glow curve temperature,
205 suggested the presence of a distribution of trapping levels (Pagonis and Michael, 1994; Rudlof et al.,
206 1978) and prompted a more detailed investigation of the kinetics of traps involved in the production
207 of TL. The application of a step heating procedure (example shown in Fig. 13a for a sample of PU
208 coated woven nylon fabric, F179PUN) confirmed a progressive shift of the TL peak to higher
209 temperatures with increasing preheat temperature, T_{stop} . Analysis of the TL glow curves using the
210 initial rise method (IRM) produced values of activation energy that increased with glow curve
211 temperature to ca 0.65 eV (Fig. 13b) at 160 °C (T_{stop}), providing further indication of the presence of
212 a distribution of energy levels. To improve the reliability of trap depth estimation in these
213 circumstances (Coleman and Yukihiro, 2018), a modified IRM procedure was applied by performing
214 beta irradiation at increasingly elevated sample temperatures to selectively block progressively
215 deeper populations of traps (Van den Eeckhout et al., 2013). In terms of trap depth variation,
216 broadly similar behaviour was observed using this procedure (Supplementary Material, Section 9,
217 Figs S6a,b), but reliable evaluation for sample temperatures above 100 °C was prevented by
218 significant statistical fluctuation in the relatively weak TL signal. Further evidence of complex trap
219 kinetics associated with the TL in this region of the glow curve were obtained by measurement of
220 the phosphorescence isothermal decay measured at elevated sample temperatures (30-180 °C), the
221 behaviour of which indicated a transfer of charge between different traps (Supplementary Material,
222 Sec. 10, Fig. S7).

223 7. Discussion

224 Fortunately, the application of quality control standards for the mass production of fabrics has led to
225 uniformity in the composition of most synthetic fabrics and this is consistent with finding similar TL
226 characteristics for samples taken from different parts of a given sampled item. However, the TL
227 sensitivity of specimens cut from synthetic fabrics incorporating filler minerals can be expected to

228 vary according to the optical transparency of the fabric, the distribution of filler and its mineral type
229 and source, and this is evident in finding a range of TL sensitivities and characteristics with different
230 fabrics.

231 The identification of carbonate rock as the source of filler grains and the presence of a strong calcite
232 signature in the XRD pattern (Fig. 3) initially suggest that the TL characteristics of the filler mineral
233 should be similar to those for calcite. On the other hand, the published TL literature on various types
234 of synthetic and natural calcite is not entirely consistent and the presence of different impurities in
235 sedimentary rock can be expected to also give rise to variations in TL characteristics, particularly in
236 the trap structure. While there are similarities in terms of the colour of emission and overall glow
237 curve shape, differences in the interpretation of trap kinetics are evident at a more detailed level.
238 Two dominant TL peaks within the temperature range 70-200 °C of the calcite glow curve (with
239 maxima located within the ranges ca 70-90 °C and 140-155 °C and referred to here as the 80 °C and
240 150 °C TL peaks, respectively) have been reported by various authors (Supplementary Material,
241 Table S3). However, a consensus value of the trap parameters associated with each of the two peaks
242 is not readily extracted from the values published for different sources of natural and synthetic
243 calcite, partly because widely differing heating rates were used (0.2-5 °C s⁻¹). For example, the 80 °C
244 TL peak has been argued by Kirsh et al. (1987) to be associated with a continuum of traps having the
245 same trap depth, but with a distribution of values of frequency factor ($T_m=82$ °C, $E=0.73$ eV; $T_m=152$
246 °C, $E=0.93$ eV; 0.33 °C s⁻¹), whereas, Kalita and Wary (2016), using curve fitting procedures with a
247 general-order kinetics equation, evaluated trap parameters for the two TL peaks assuming two
248 conventionally discrete traps ($T_m=87$ °C, $E=0.60$ eV; $T_m=137$ °C, $E=1.3$ eV; 2 °C s⁻¹). Similarly, Kim and
249 Hong (2014), testing a natural calcite sample, used curve fitting procedures to identify the presence
250 of the 80 °C and 150 °C TL peaks within a very broad glow peak extending from ca 50 C to 200 °C. On
251 the basis of estimated E (0.92 eV) and s (0.92×10^9 s⁻¹) values they calculated a lifetime (15 °C) of 32h
252 for the higher temperature peak (Supplementary Material, Table S3). The results obtained using the
253 $T_{\max}-T_{\text{stop}}$ method are presented here to illustrate the complex nature of the trap population in the

254 filler grains examined rather than to extract accurate estimates of trap depth. Given the nature of
255 the samples and the consequent issues of thermal lag, more detail experiments are required using
256 filler grains extracted from their polymer host.

257 Hence, on the basis of the analysis of initial rise (IR) and isothermal fading measurements, the results
258 obtained with fabric samples appear to present a set of mixed correlations with the above
259 interpretations of trap structure and estimated energy levels previously reported for calcite. While
260 the issue of trap structure, which is likely to vary between different mineral sources, requires further
261 investigation, the trap parameters and mean lifetime estimates obtained from isothermal decay
262 measurements for the example shown (PU coated nylon, HB16PU, Table 1) for the 158-160 °C glow
263 curve interval more closely resemble the lifetime for the 150 °C TL peak by calculated by Kim and
264 Hong (2014) for their natural calcite sample. The indications of a distribution of trap energy levels
265 associated with the high temperature tail of the broad peak that extends to nearly 200 °C appears to
266 be similar to that proposed by Kirsh et al. (1987) for the lower 80 °C TL peak.

267

268 As indicated in Fig. 11, significant differences in the rate of fading at ambient temperatures were
269 observed between the various fabric samples tested. Although changes in thermal lag between
270 samples (5-10 °C), are expected to give rise to different relative reductions at a given glow curve
271 temperature between fabrics of differing thicknesses and thermal conductivities, an examination of
272 the set of samples tested indicate varying proportions of two or more fading components and this is
273 likely to be associated with specific mineral type and source. The data collected from the storage
274 tests are sufficient to indicate that the fading of a sample extracted from a commercially produced
275 fabric containing a carbonate filler cannot be assumed to follow the characteristic form for a single
276 energy trap associated with calcite and that sample-specific measurements to characterise short-
277 term fading behaviour are necessary. As the fading behaviour of the high temperature tail of the
278 glow curve indicates a process of charge loss that is dominated by a thermal escape mechanism, the

279 temporal range of use of the higher temperature region of the TL glow curve for dosimetry can be
280 extended by storage at reduced temperatures. Whereas the loss of the TL signal (158-160 °C)
281 following beta irradiation was typically 50% following 24h storage at ambient temperatures (20 °C),
282 the results of the storage measurements performed at -15 °C indicated (Fig. 12) that the loss was
283 reduced to less than 10 % over several days following irradiation. Nonetheless, the application of
284 corrections for fading following irradiation and storage at ambient temperatures has been found to
285 be practicable, yielding a satisfactory equivalent dose plateau within the glow curve interval 140-160
286 °C (Fig. 14). At higher glow curve temperatures (>160 °C), the relatively weak TL signal was found to
287 limit the precision of absorbed dose estimates within the dose range of interest (0.1-10 Gy).

288 As noted above, a native TL signal observed with some samples was substantially reduced by the
289 insertion of a sharp cut optical filter in the detection system to block wavelengths shorter than 550
290 nm. Measurement of the TL glow curve with extracted filler grains revealed a peak located at ca 250
291 °C, the low temperature tail of which extends to below 200 °C in the glow curve. This TL signal arises
292 from the cumulative natural environmental dose and is referred to as the 'native' signal. This peak is
293 also observed in calcite (Wintle, 1978; Kirsh et al., 1987) and its strong attenuation by insertion of
294 the sharp cut filter suggests the presence of the shorter wavelength emission present in the CL
295 emission spectrum of the filler grains, and it is also observed in the TL emission spectrum of calcite
296 (Down et al. 1985; Townsend et al., 1994). However, it should be noted that the generation of a non-
297 radiation-induced 'spurious' TL signal by crushing (triboluminescence) and exposure to air is a well-
298 known effect in calcite (Wintle, 1975). Although the TL response of the fabric samples tested was not
299 found to be sensitive to exposure in air, precautionary tests should be performed to confirm this.

300 In terms of the potential suitability of previously untested fabrics, two experimental issues of
301 primary interest are a) whether the TL sensitivity is sufficient for the dose range of interest and b)
302 the correction factors to be applied for fading. Of the fabric types tested, the detection limit for the
303 majority of samples was found to be sufficiently low for the determination of absorbed dose of

304 above ca 100 mGy using cut samples (to fit within 10 mm dia. measurement pans). The extent of
305 inter-and intra-sample variability in TL sensitivity observed, as discussed above, requires that the
306 dose response is established. If good characteristics in terms of linearity, absence of sensitization
307 and a small dose intercept are similarly found with wider testing, it may prove acceptable to limit
308 investigation of the dose response to measurement at one dose point. On the basis of tests
309 performed with different samples taken from the same fabric, the fading characteristics of individual
310 samples taken from the same accessory or garment are expected to be similar. However, sample-
311 specific fading measurements are required to determine the coefficient(s) of the exponential decay.
312 As discussed above, a reduction in the storage temperature provides the opportunity to substantially
313 lower the trapped charge loss by promptly storing fabrics at a reduced temperature, such as in a
314 domestic freezer, following exposure to ionising radiation.

315 Where filler grains in the surface of a fabric are exposed daylight (e.g., faux leather), optical fading is
316 potentially a further issue. In addition to finding negligible bleaching tests under laboratory white
317 light illumination of up to 5h, the absence of significant bleaching effects was also observed in a
318 radiation simulation experiment, where a 'blind' gamma dose was administered to bags mounted on
319 a phantom under artificial and subsequently daylight lighting conditions before transfer to the
320 laboratory for measurement (Bossin et al., forthcoming). However, given the complex behaviour of
321 traps in the calcite structure discussed above, a more detailed investigation of the behaviour of the
322 TL peaks below 200 °C under more demanding illumination conditions (e.g., intense sunlight) is
323 required. In the case of backpacks the filler-bearing film is typically found on the inner surface of the
324 nylon fabric and hence the issue of optically-induced effects following irradiation is less problematic.
325 Similarly, in the case of faux leather handbags, samples from interior optically shielded locations are
326 usually available. Nonetheless, as phototransfer effects in calcite under short UV (<300 nm)
327 illumination have been reported (Lima et al., 1990) with a peak at ca 180 °C (Liritzis et al., 1996), the
328 full extent of the influence of UVA in intense natural sunlight requires further investigation.

329 Conclusion

330 In this study we have shown that the presence of granular mineral carbonate fillers commonly added
331 in the manufacture of synthetic fabrics, in particular those used in the manufacture of clothing
332 accessories such as handbags and backpacks, provides the opportunity to apply TL measurement
333 techniques to obtain determinations of absorbed dose. Using cut specimens (which do not require
334 the extraction of the mineral grains), the TL response to absorbed dose was found to be sufficiently
335 high to provide a detection limit of better than ca 100 mGy for the majority of fabrics tested in the
336 study, with a linear response to (β) radiation dose that is well beyond the range of interest (ca 0.1-10
337 Gy) required to support medical triage. Although the detailed fading behaviour varies according to
338 fabric type and the mean lifetime of traps is relatively short compared with conventional dosimeter
339 phosphors, the shortest being ca 18 h at 20 °C, a test of the reliability of corrections for fading has
340 been successfully completed in a blind gamma dose irradiation exercise performed with fabrics
341 maintained at ambient temperatures (Bossin et al., in preparation). Moreover, the useful temporal
342 range for dose measurements can be extended significantly by storage of the fabrics at a reduced
343 temperature following irradiation. The use of mineral fillers in polymer-based materials opens up a
344 much wider scope for investigation of their suitability as a surrogate dosimetry material, providing
345 the opportunity to obtain greater flexibility in the positions available for dose determinations to
346 individuals following a radiological emergency.

347 Acknowledgments

348 The work presented here formed part of a PhD project (LB) sponsored by Public Health
349 England and Durham University, LB's non-academic supervisors were Dr. R. Tanner and Dr. J. Eakins
350 of the Radiation Metrology group and Dr. E. Ainsbury of the Cytogenetics Group, Public Health
351 England. The authors would like to thank Mr. G. Oswald (Chemistry Department, Durham University)
352 for performing the XRD measurements. The EMCCD images were taken at the Luminescence
353 laboratory of the University of Lausanne.

354

355 **References**

356 Ainsbury, E.A., Bakhanova, E., Barquinero, J.F., Brai, M., Chumak, V., Correcher, V., Darroudi, F.,
357 Fattibene, P., Gruel, G., Guclu, I. and Horn, S. (2010). Review of retrospective dosimetry techniques
358 for external ionising radiation exposures. *Radiation Protection Dosimetry*, 147(4), 573-592.

359 Bailiff, I. K., Sholom, S., McKeever, S. W. S. (2016). Retrospective and emergency dosimetry in
360 response to radiological incidents and nuclear mass-casualty events: a review. *Radiation*
361 *Measurements*, 94, 83-139.

362 Bassinet, C., Woda, C., Bortolin, E., Della Monaca, S., Fattibene, P., Quattrini, M.C., Bulanek, B.,
363 Ekendahl, D., Burbidge, C.I., Cauwels, V. and Kouroukla, E., E. (2014). Retrospective radiation
364 dosimetry using OSL of electronic components: results of an inter-laboratory comparison. *Radiation*
365 *Measurements*, 71, 475-479.

366 Bossin, L., Bailiff, I. K., Terry, I. (2017). Luminescence characteristics of some common polyester
367 fabrics: Application to emergency dosimetry. *Radiation Measurements*, 106, 436-442.

368 Bossin, L., Bailiff, I. K., Terry, I., Tanner, R., Eakins, J., Ainsbury, L. Radiological emergency dosimetry
369 using mineral fillers: results from a blind test. Submitted to *Radiation Measurements*.

370 Coleman, C.N., Weinstock, D.M., Casagrande, R., Hick, J.L., Bader, J.L., Chang, F., Nemhauser, J.B. and
371 Knebel, A.R. (2011). Triage and treatment tools for use in a scarce resources-crisis standard of care
372 setting after a nuclear detonation. *Disaster medicine and public health preparedness*, 5(S1), S111-
373 S121.

374 Coleman, A. C., Yukihiro, E. G. (2018). On the validity and accuracy of the initial rise method
375 investigated using realistically simulated thermoluminescence curves. *Radiation Measurements*, 117,
376 70-79.

- 377 Down, J. S., Flower, R., Strain, J. A., Townsend, P. D. (1985). Thermoluminescence emission spectra
378 of calcite and Iceland spar. *Nuclear Tracks and Radiation Measurements (1982)*, 10(4-6), 581-589.
- 379 Ekendahl, D., Judas, L. (2011). Retrospective dosimetry with alumina substrate from electronic
380 components. *Radiation Protection Dosimetry*, 150(2), 134-141.
- 381 Folk, R. L. (1962). Spectral subdivision of limestone types. In: (Ed. W.E. Ham, W.E.) Classification of
382 Carbonate Rocks. American Association of Petroleum Geology Memoir No. 1, Tulsa, OK, pp. 62-84.
- 383 Galloway, R. B. (2002). Does limestone show useful optically stimulated luminescence? *Ancient TL*,
384 20(1), 1-5.
- 385 Inrig, E. L., Godfrey-Smith, D. I., Khanna, S. (2008). Optically stimulated luminescence of electronic
386 components for forensic, retrospective, and accident dosimetry. *Radiation Measurements*, 43(2-6),
387 726-730.
- 388 Kalita, J. M., Wary, G. (2014). Thermoluminescence study of X-ray and UV irradiated natural calcite
389 and analysis of its trap and recombination level. *Spectrochimica Acta Part A: Molecular and*
390 *Biomolecular Spectroscopy*, 125, 99-103.
- 391 Kalita, J. M., & Wary, G. (2016). X-ray dose response of calcite—a comprehensive analysis for optimal
392 application in TL dosimetry. *Nuclear Instruments and Methods in Physics Research Section B: Beam*
393 *Interactions with Materials and Atoms*, 383, 93-102
- 394 Katz, H. S., Mileski, J. V. (Eds.). (1987). *Handbook of fillers for plastics*. Springer Science & Business
395 Media.
- 396 Kim, K. B., Hong, D. G. (2014). Kinetic parameters, bleaching and radiation response of
397 thermoluminescence glow peaks separated by deconvolution on Korean calcite. *Radiation Physics*
398 *and Chemistry*, 103, 16-21.

- 399 Kirsh, Y., Townsend, P. D., Shoval, S. (1987). Local transitions and charge transport in
400 thermoluminescence of calcite. *International Journal of Radiation Applications and Instrumentation.*
401 *Part D. Nuclear Tracks and Radiation Measurements*, 13(2-3), 115-119.
- 402 Kouroukla, E. (2015). Luminescence dosimetry with ceramic materials for application to radiological
403 emergencies and other incidents (Unpublished doctoral thesis, Durham University).
- 404 Lafuente, B., Downs, R. T., Yang, H., Stone, N. (2016). The power of databases: the RRUFF project. In
405 *Highlights in mineralogical crystallography* (pp. 1-29). Walter de Gruyter GmbH.
- 406 Lima, J. F., Trzesniak, P., Yoshimura, E. M., & Okuno, E. (1990). Phototransferred
407 thermoluminescence in calcite. *Radiation Protection Dosimetry*, 33(1-4), 143-146.
- 408 Liritzis, I., Guibert, P., Foti, F., & Schvoerer, M. (1996). Solar bleaching of thermoluminescence of
409 calcites. *Nuclear Instruments and Methods in Physics Research Section B: Beam Interactions with*
410 *Materials and Atoms*, 117(3), 260-268.
- 411 Medlin, W. L. (1959). Thermoluminescent properties of calcite. *The Journal of Chemical Physics*,
412 30(2), 451-458.
- 413 Pagonis, V., Michael, C. (1994). Annealing effects on the thermoluminescence of synthetic calcite
414 powder. *Radiation Measurements*, 23(1), 131-142.
- 415 Pagonis, V., Allman, E., & Wooten Jr, A. (1996). Thermoluminescence from a distribution of trapping
416 levels in UV irradiated calcite. *Radiation Measurements*, 26(2), 265-280.
- 417 Rudlof, G., Becherer, J., & Glaefcke, H. (1978). Behaviour of the fractional glow technique with first-
418 order detrapping processes, traps distributed in energy or frequency factor. *Physica Status Solidi (a)*,
419 49(2), K121-K124.
- 420 Schulman, J. H., Evans, L. W., Ginther, R. J., & Murata, K. J. (1947). The Sensitized Luminescence of
421 Manganese-Activated Calcite. *Journal of Applied Physics*, 18(8), 732-739.

- 422 Sunta, C. M. (1984). A review of thermoluminescence of calcium fluoride, calcium sulphate and
423 calcium carbonate. *Radiation Protection Dosimetry*, 8(1-2), 25-44.
- 424 Townsend, P. D., Luff, B. J., & Wood, R. A. (1994). Mn²⁺ transitions in the TL emission spectra of
425 calcite. *Radiation Measurements*, 23(2-3), 433-440.
- 426 Van den Eeckhout, K., Bos, A. J., Poelman, D., & Smet, P. F. (2013). Revealing trap depth distributions
427 in persistent phosphors. *Physical Review B*, 87(4), 045126.
- 428 Wintle, A. G. (1975). Effects of sample preparation on the thermoluminescence characteristics of
429 calcite. *Modern Geology*, 5, 165-167.
- 430 Wintle, A. G. (1978). A thermoluminescence dating study of some Quaternary calcite: potential and
431 problems. *Canadian Journal of Earth Sciences*, 15(12), 1977-1986.
- 432 Woda, C., Fiedler, I., & Spöttl, T. (2012). On the use of OSL of chip card modules with molding for
433 retrospective and accident dosimetry. *Radiation Measurements*, 47(11-12), 1068-1073.
- 434 Wypych, G. (2016). *Handbook of Fillers*. Elsevier.

435

Radiological emergency dosimetry – the use of luminescent mineral fillers in polymer-based fabrics

Table

Table 1. Values of kinetic parameters calculated using the isothermal decay method in different integration regions of the TL glow curve measured with a sample of faux leather (HB16PU). The uncertainties in the value of E reflect fitting errors only.

Method	Temp region (°C)	Activation energy (eV)	Frequency factor, s (s ⁻¹)	Calculated lifetime at 20 °C (h)	Calculated TL remaining, 24 h at 20 °C (%)	Measured TL remaining, 24 h at 20 °C (%)
Isothermal Decay	140-142	0.81±0.08	3.0×10 ⁹	8	5	14
	158-160	0.91±0.02	6.6×10 ¹⁰	18	27	25
Initial Rise ¹	145 ³	0.54	5.8×10 ⁴	9	7.5	16
Initial Rise ²	165 ³	0.65	5.9×10 ⁵	71	71	29

¹ T_{max}-T_{stop}, preheat: 170 °C

² β irradiation at elevated temperature (130 °C)

³ Peak maximum position

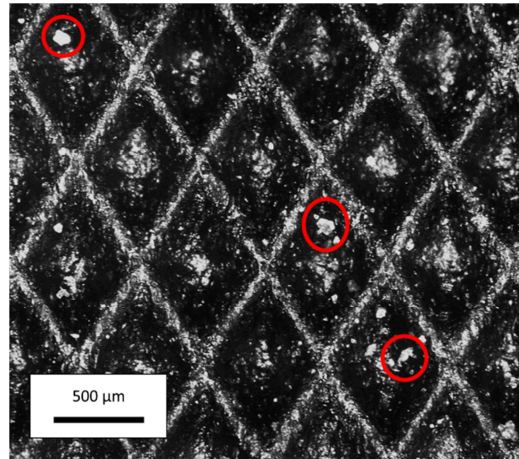


Fig. 1. Image of the PU coating of a nylon fabric (BPLEDPUN) obtained using an optical microscope. Several mineral filler grains are circled in red; examination of extracted grains using XRD and SEM analysis indicated that the source material was unweathered crushed limestone. The repeated diamond pattern is the plastic imprint.

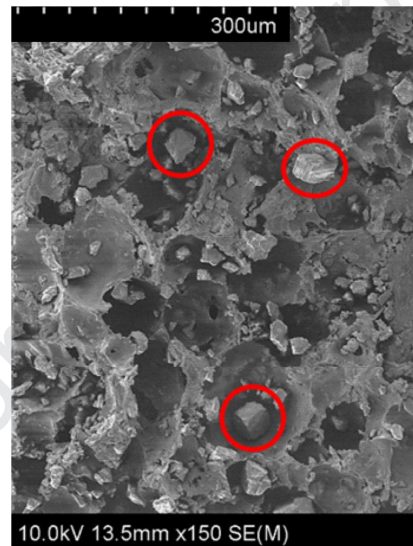


Fig. 2. SEM image of a sample of faux leather (HB16PU) identifying, amongst others, three calcium carbonate filler grains (encircled in red). The sample was coated with 10 nm of gold. Electron beam: 10 kV.

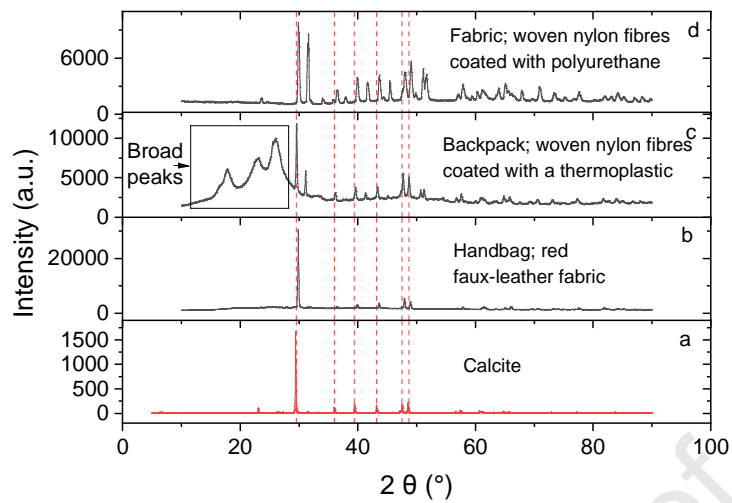


Fig. 3. XRD patterns: a) calcite; b) faux leather (HB16PU); c) PU coated nylon (BP21PUN); d) PU coated nylon (F179PUN). The broad peaks observed at low angles are attributed to polymer (within square in c). The broken lines indicate the position of some of the characteristic peaks of calcite. The XRD pattern of calcite (Tie Sidings, USA) was obtained from the RRUFF database (Lafuente et al., 2016).

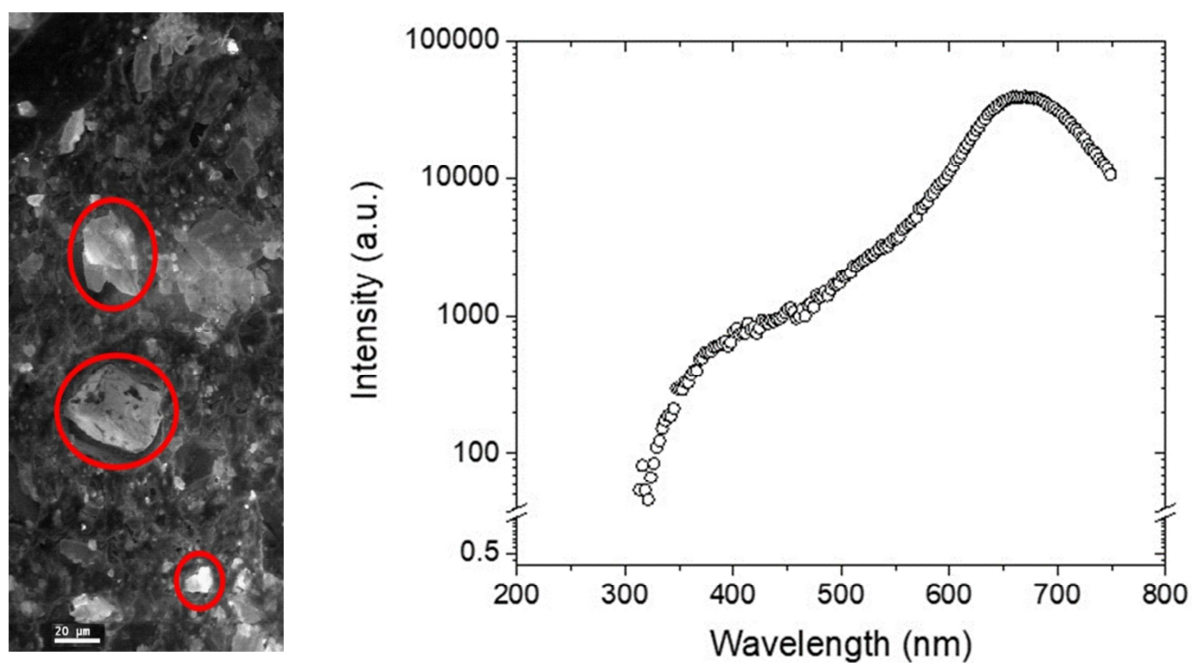


Fig. 4. a) CL image of a sample of PU coated nylon fabric (BPLEDPUN), coated with 10 nm of platinum, electron beam 10 kV, CL detector spectral range: 185-850 nm. The red circles identify three of the luminescing carbonate filler grains amongst numerous other smaller grains in the image. b) A spatially averaged CL emission spectrum obtained with a sample of the same fabric (BPLEDPUN), where the spectrum is corrected for instrument response.

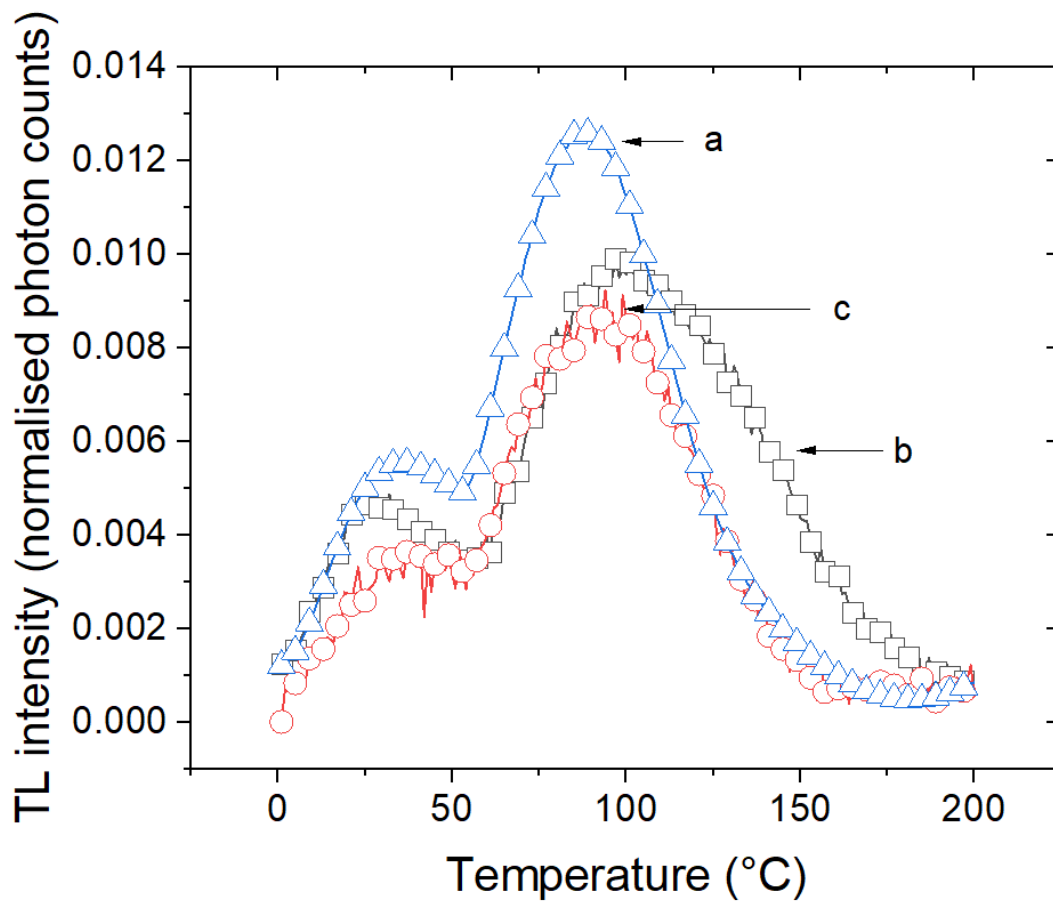


Fig. 5. TL glow curves following β dose measured with a) limestone grains, b) PU coated nylon fabric (LEDBPPUN) and c) filler grains extracted from the fabric coating and deposited onto a stainless steel measurement disc. Detection: PMT, EMI 9235 with silica window; heating rate: $0.5 \text{ }^\circ\text{C}\cdot\text{s}^{-1}$. The TL intensity of each glow curve corresponds to the photon count (per 2s intervals) normalised by the integrated photon count.

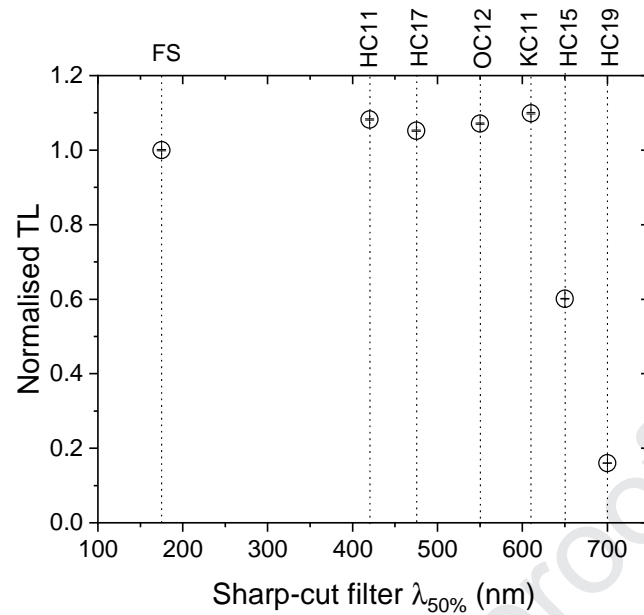


Fig. 6. Integrals of the TL glow curve region 140-160 °C for samples of faux leather (HB16PU) following β irradiation (1 Gy) measured using different sharp-cut filters. The x axis indicates the wavelength above which the transmission of the filter is 50% ($\lambda_{50\%}$). The TL integrals were normalised to the TL signal measured using a fused silica (FS) window (> 175 nm). PMT: Hamamatsu R2949; Optical filters and their sharp cut wavelengths; HC11 (above ~ 400 nm), HC17 (above ~ 500 nm), OC12 (above ~ 550 nm), KC11 (above ~ 600 nm), KC 15 (above ~ 650 nm) and KC 19 (above ~ 700 nm).

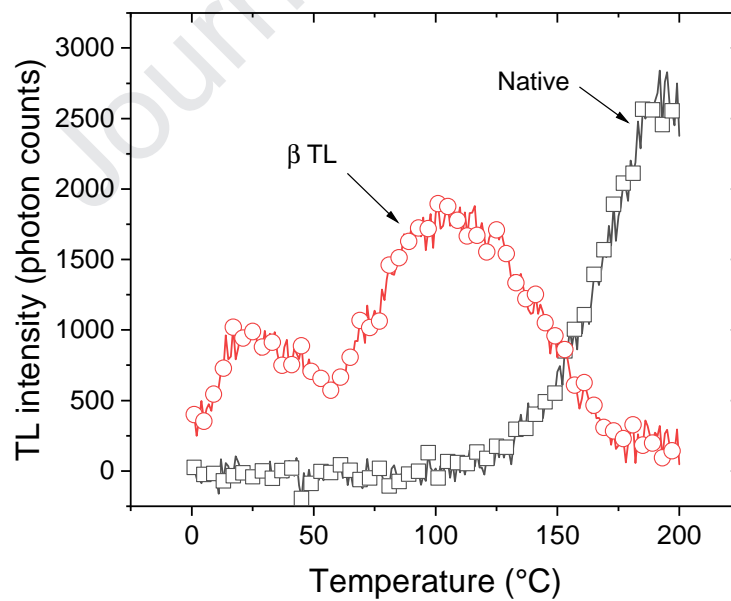


Fig. 7. Native TL (open squares) and TL measured following a β dose (1 Gy, open circles) administered to a sample of PU coated nylon (HB5PUN). PMT: EMI 9235; detection window: fused silica window, heating rate: $0.5 \text{ }^\circ\text{C}\cdot\text{s}^{-1}$, no preheat.

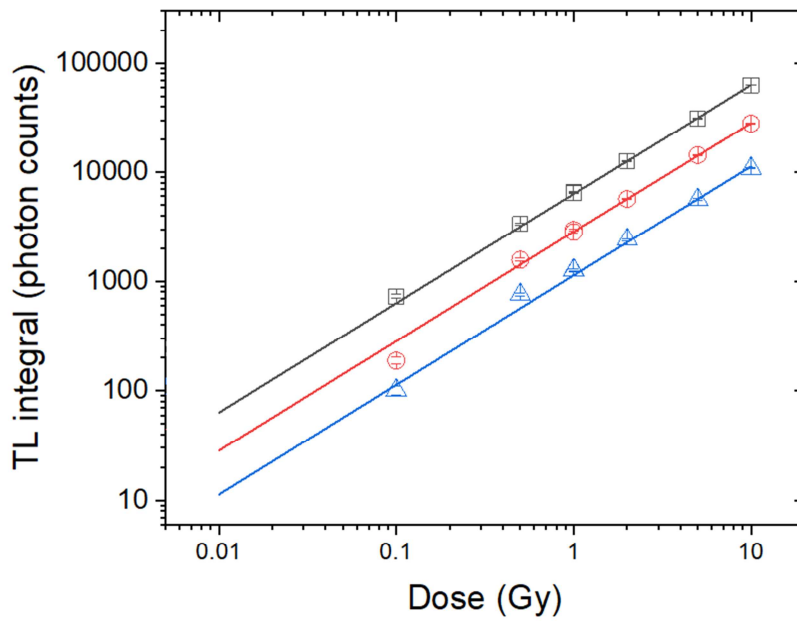


Fig. 8. TL dose response characteristics measured with a sample of PU coated nylon (BP21PUN) following the administration of β doses in the range indicated, shown for three glow curve integration regions: 105-135 °C (open black squares), 140-160 °C (open red circles) and 160-175 °C (open blue triangles). A linear function was fitted to the experimental data. PMT: Hamamatsu R2949; Detection optical filter: OC12.

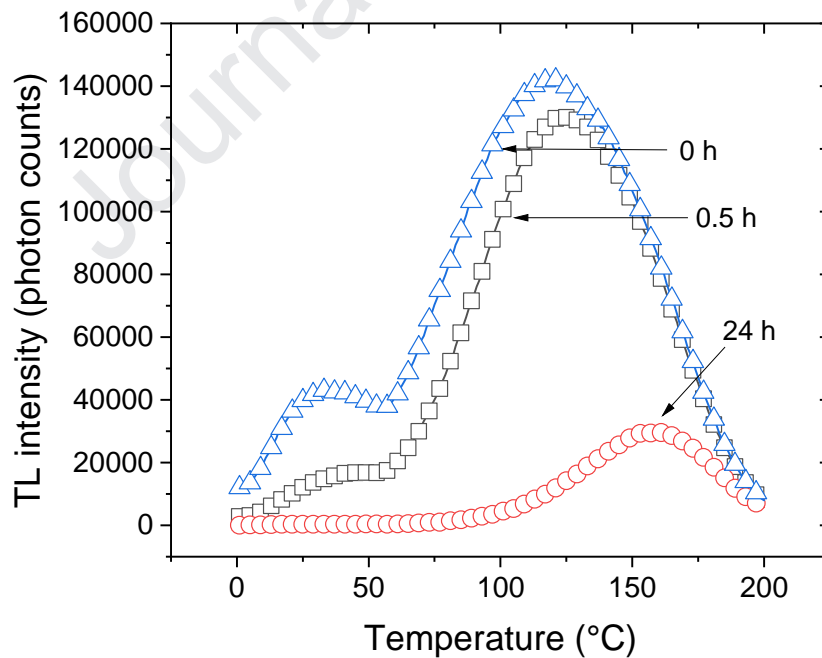


Fig. 9. TL glow curves measured with a sample of PU coated nylon (HB21PU) following β irradiation (10 Gy) and storage in the dark at room temperature for: 0 h (open blue triangles), 0.5 h (open black squares) and 24 h (open red circles). PMT: Hamamatsu R2949; Detection optical filter: OC12; Heating rate: $0.5\text{ }^{\circ}\text{C}\cdot\text{s}^{-1}$.

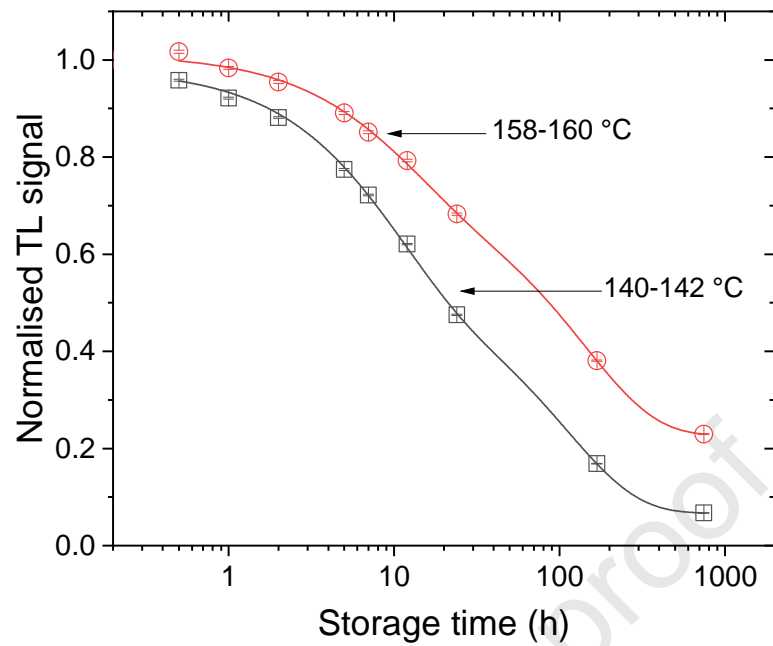


Fig. 10. Remaining TL signal following β irradiation and storage in the dark at room temperature (0.5-744 h), measured with a sample of PU coated nylon (F179PUN). The remaining TL signal was calculated as the integral in the region 140-142 °C (open black squares) and 158-160 °C (open red circles) and normalised to the TL signal measured promptly following the irradiation (≤ 5 min). The continuous lines indicate stretched exponential functions fitted to the experimental data. Detection window: fused silica window; Heating rate: $0.5 \text{ }^\circ\text{C}\cdot\text{s}^{-1}$, PMT: R2949.

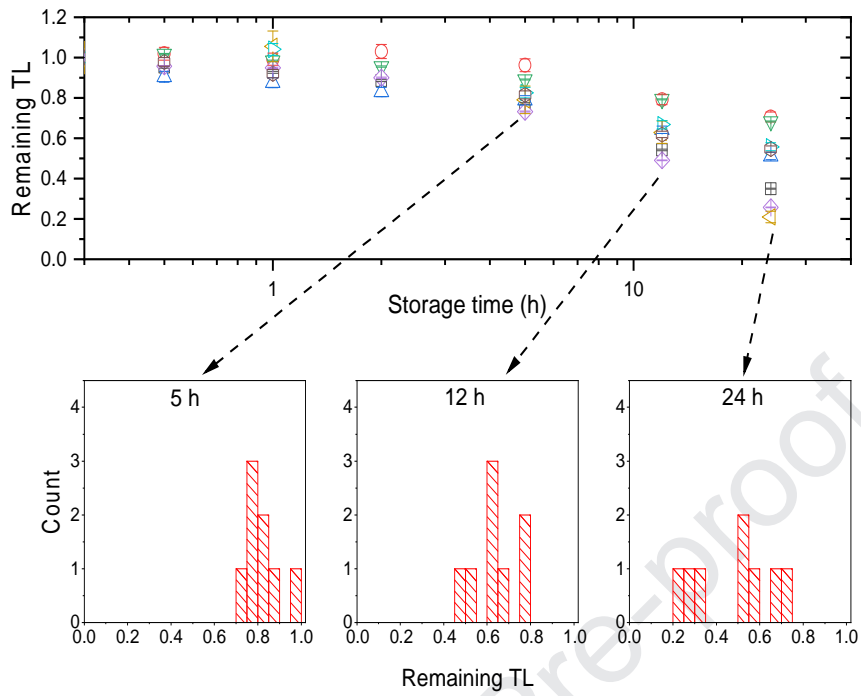


Fig. 11. Remaining TL signal following β irradiation and storage in the dark at room temperature for various periods (0.5-24 h), measured with the following samples: faux leather (HB19PU, black squares; HB16PU, purple diamonds), PU coated nylon backpack fabric (BP21PUN, red circles; BP11PUN, blue triangles), PU coated nylon fabric swatches (F179PUN, green inverted triangles; F202PUN, turquoise triangles; F213PUN, brown circles) and PU coated nylon conference bag fabric (CBRPWPUN, brown triangles). The remaining TL corresponds to the TL signal calculated as the integral in the region 158-160 °C normalised to the TL signal measured promptly following β irradiation (≤ 5 min). The histograms indicate the distribution of the proportions of remaining TL for all samples after 5 h, 12 h and 24 h of storage. Detection: Hamamatsu R2949 PMT with OC 12 optical filter. Heating rate: $0.5 \text{ }^\circ\text{C s}^{-1}$.

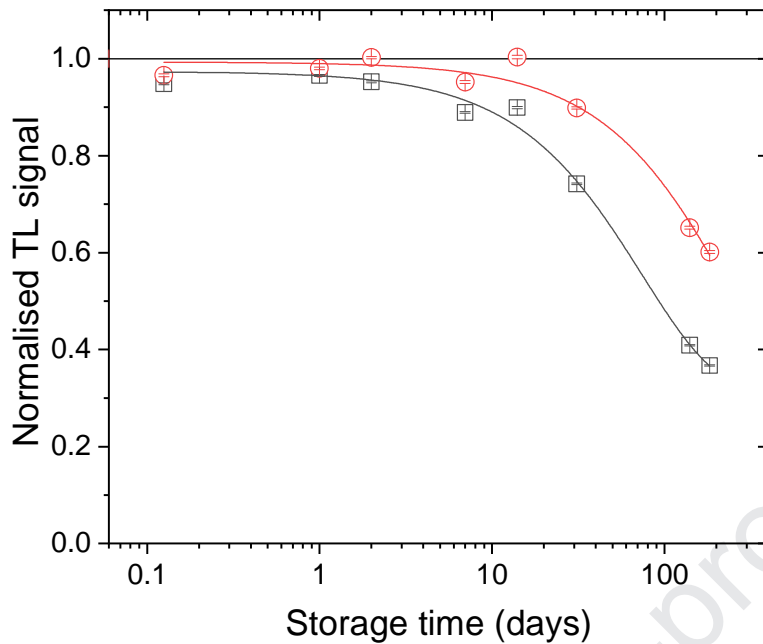


Fig.12 . Remaining TL following β irradiation (10 Gy) and storage in the dark at $-15\text{ }^{\circ}\text{C}$ for various storage periods (0.125-183 days) measured with a sample of PU coated fabric swatch (F179PUN). The remaining TL signal was calculated as the integral in the region $140\text{-}142\text{ }^{\circ}\text{C}$ (open black squares) and $158\text{-}160\text{ }^{\circ}\text{C}$ (open red circles) and normalised to the TL signal measured promptly following β irradiation (≤ 5 min). The horizontal line indicates the absence of fading ($\gamma=1$) and the continuous lines represent single stretched exponential functions fitted to the experimental data. Detection: PMT Hamamatsu R2949 with optical filter OC12. Heating rate: $0.5\text{ }^{\circ}\text{C s}^{-1}$. The TL intensity was similar to that of samples stored at room temperature following β irradiation.

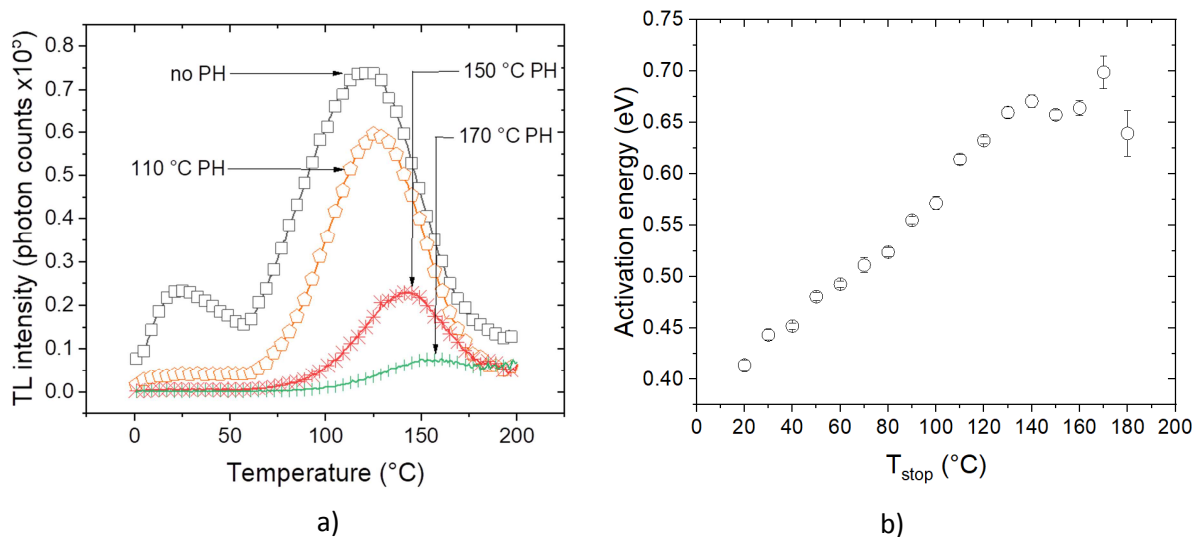


Fig. 13. a) Glow curves obtained applying the $T_{\max}\text{-}T_{\text{stop}}$ method to a sample of PU coated nylon (F179PUN), where the following treatments were applied: No preheat (open black squares); $110\text{ }^{\circ}\text{C}$ (open orange polygons); $150\text{ }^{\circ}\text{C}$ (red stars) and $170\text{ }^{\circ}\text{C}$ (green bars). Preheat: cut-heat; PMT: Hamamatsu R2949 with additional fused silica window; heating rate: $0.5\text{ }^{\circ}\text{C.s}^{-1}$. b) Activation energies were calculated applying the initial rise method to the sample following β irradiation (1 Gy) and heating to the selected cut-heat, T_{stop} , in the range $20\text{-}180\text{ }^{\circ}\text{C}$.

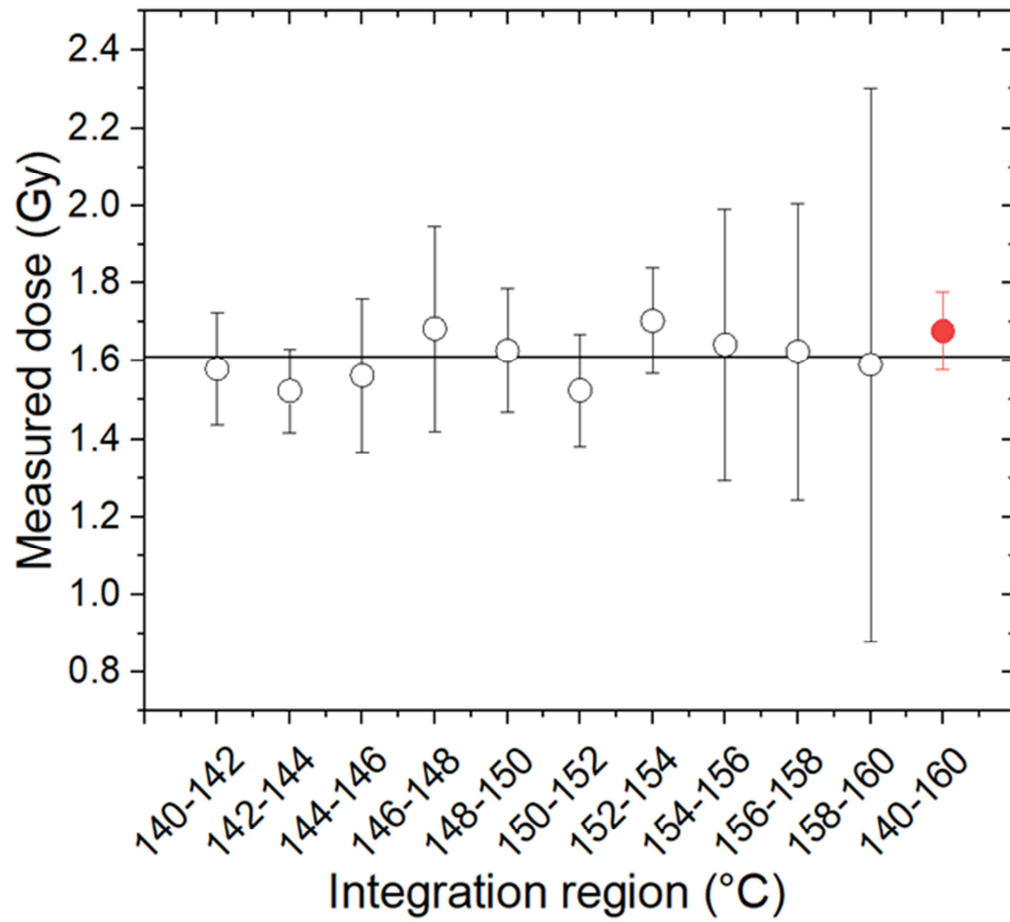


Fig. 12. Plateau test performed with a sample cut from bag BP21PUN. The value of dose was calculated as $I_T * f / m$, where I_T is the signal recorded in the interval T (2 °C) divided by the gradient m of the dose response curve and f is the interval-specific fading correction applied. The TL signal of the reconstructed dose was measured 6 hours following irradiation.

Highlights

- Mineral fillers widely used in the manufacture of thermoplastic exhibit a bright thermoluminescence (TL) signal.
- Mineral fillers are commonly found in the fabric of bags and their TL response can be used for emergency dosimetry.
- Their signal yields a linear dose response in the range 0.1-10 Gy with detection limits from 4 to 400 mGy.
- The fading is sample dependent but can be circumvented by storing the samples at low temperature (-15 °C) .

Journal Pre-proof

Declaration of interests

The authors declare that they have no known competing financial interests or personal relationships that could have appeared to influence the work reported in this paper.

The authors declare the following financial interests/personal relationships which may be considered as potential competing interests: